Rapid Thermal Energy Modeling and Analysis of Complex Industrial Hydraulic Systems

Ahmad Al-Issa*, Tobias Schulze and Jürgen Weber

Chair of Fluid-Mechatronic Systems, TU Dresden, Dresden, Germany
E-mail: ahmad.alissa.85.85@gmail.com
**Corresponding Author*

Received 01 November 2024; Accepted 05 February 2025

Abstract

Modeling and analyzing the thermal energy behavior of industrial hydraulic systems with useful hydraulic power of 20 kW or higher is a challenging task due to the system's inherent complexity and the multitude of interacting components. Conventional thermal modeling approaches rely heavily on numerous interdependent parameters and sensor measurements, including temperature, pressure, and flow rate for each port in hydraulic component. This reliance often leads to prolonged modeling times, which can exceed the actual operational time of the hydraulic system by a factor of 2 to 6.5, resulting in costly and time-intensive analysis. To address these limitations and meet industrial demands, this study introduces an enhanced thermal model based on a new temperature parameter, termed the average transient temperature ($\mathrm{T_{avg}}$), aimed at significantly reducing the modeling time to be shorter than the experimental operation time. Furthermore, Physics informed neural network model is used to determine hydraulic oil specifications during the modeling implementation as one correlation model.

Keywords: Industrial hydraulic system, thermal energy model, reduction of modeling time, thermodynamics.

International Journal of Fluid Power, Vol. 26_1, 65–98.
doi: 10.13052/ijfp1439-9776.2614

1 Introduction

Since the 1990s, interest in modeling and analyzing hydraulic system performance has steadily increased. Harris (1990) [1] pioneered a thermodynamic analysis approach for predicting temperature variations resulting from individual components or component groups. Subsequently, Sidders et al. (1996) [2] presented a method for analyzing both the transient and steady-state thermal hydraulic performance of fluid power systems. They explored the theoretical basis and modeling techniques for an open circuit consisting of a hydraulic pump, load valve, heat exchanger, and reservoir.

Zhang, 2011 [3] investigated the thermal behavior of aircraft hydraulic systems by analyzing heat generation and dissipation, and developing a detailed formula for temperature variation. Busquets, 2013 [4] developed a comprehensive mathematical model to predict the thermodynamic behavior of displacement controlled multi-actuator machines, significantly improving energy efficiency by eliminating metering losses.

Chenggong and Zongxia (2008) [5] introduced fundamental approaches for modeling thermal-hydraulic components using lumped parameter mathematical sets. They also discussed integration methods for solving cross-coupled thermal-hydraulic equations in position-controlled thermal-hydraulic systems. Their thermal-hydraulic simulation showed a minimum elapsed time of 32.7 seconds for a 5-second experiment, equating to 6.5 times the actual operational duration. More recent studies by Li et al. (2014) [6], Michel (2021) [7], and Ketelsen et al. (2021) [8] have developed thermal-hydraulic models by analyzing heat transfer and applying the lumped-parameter method to hydraulic components in Electro-Hydrostatic Actuators (EHA). In Ketelsen et al.'s work, the simulation time was twice the actual operational duration, with a time step of 2×10^{-4} seconds for the simulation.

Kwon et al. (2016) [9] investigated the thermal characteristics of hydraulic hybrid vehicle (HHV) transmissions through a thermodynamic analysis. A simulation model combining hydraulic and thermal system models was developed to analyze the performance of a closed-circuit hydraulic hybrid transmission. The research presented by Siddiqui et al. (2022) [10] addressed the critical issue of overheating in an electro-hydraulically operated machine used in underground mining. They utilized mathematical models and experimental studies to assess the causes of heat generation and inefficiencies in the hydraulic components.

Previous research on time-dependent thermal models indicates that accurate modeling and analysis necessitate the consideration of at least three

primary variables – temperature, pressure, and volume flow rate – at each port (e.g., inlet, outlet) of hydraulic component. The need for numerous sensors to validate these parameters adds complexity to the experimental setup and data acquisition process. Moreover, this dependency on extensive sensor data significantly prolongs the modeling duration, often extending it by a factor of 2 to 6.5 times the actual experimental runtime for time steps of 2×10^{-4} seconds or smaller, thereby increasing both computational time and associated resource costs.

In today's context, where global warming is a pressing concern, any innovation that reduces energy consumption is highly valuable in addressing this challenge. Within the field of industrial hydraulic systems, one such proposed approach is to accelerate the modeling and analysis process during the design phase while accurately capturing the system's thermal energy behavior over a defined operational period. This study introduces an improved and rapid method for transient thermal modeling and analysis, validated through an industrial case study. Moreover, to the best of our knowledge, no existing literature offers a direct method for assessing the thermal condition of a hydraulic system under overheating conditions. Therefore, this critical aspect is also incorporated into our approach.

2 Industrial Hydraulic System

The experimental work of this study is conducted on an industrial hydraulic system utilized in an aluminum hot rolling mill for the production of aluminum alloy strips. The machine and its hydraulic system were designed and manufactured by SMS group GmbH. Figure 1 shows a simplified structure diagram of a hot rolling mill.

The industrial hydraulic system consists of several units as follows:

1. Pump Station
2. Cooling Unit
3. Accumulators Unit
4. Hydraulic Gap Control Cylinders Unit
5. Positive Bending Cylinders Unit
6. Negative Bending Cylinders Unit
7. Balancing Cylinders Unit

Each unit within the hydraulic system is designed for a specific function and comprises multiple hydraulic components, as illustrated in the following figures and detailed in Table 1. The pump station and its associated cooling

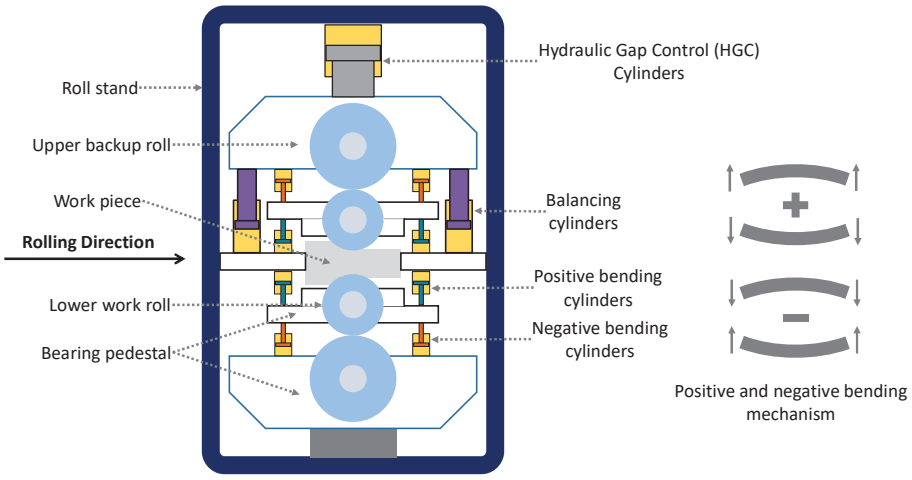

Figure 1 Simplified structure diagram of a hot rolling mill.

unit, depicted in Figure 2, incorporate three axial piston variable pumps capable of operating at a maximum pressure of 292 bar. These pumps provide hydraulic power to the rolling mill machine's actuators and the accumulator unit. The cooling unit regulates the hydraulic oil temperature, maintaining it within an acceptable range of approximately 42°C to 50°C. It activates when the oil temperature exceeds 50°C and deactivates once it drops to 42°C.

The accumulator unit uses three hydraulic accumulators to store hydraulic oil at a pressure of 220 bar. This is critical for maintaining system pressure, storing and releasing energy, and absorbing pressure spikes.

The load side of the mill machine consists of four main hydraulic cylinder subunits: Hydraulic Gap Control (HGC) (Figure 3), positive bending (Figure 4), negative bending (Figure 5), and balancing (Figure 6). Each of the first three subunits includes cylinders positioned on both the drive side (DS) and the operator side (OS) of the mill machine. Hydraulic oil flow to these cylinder units is precisely regulated by a proportional directional control valve (DCV). These subunits are equipped with pressure sensors and servo valve opening signals, which are critical for determining the flow rate. Additionally, only the HGC cylinders are fitted with displacement sensors.

All these units are situated in a well-ventilated area to ensure unrestricted airflow, with the ambient temperature maintained within a range of approximately 15°C to 35°C. The hydraulic system operates using HLP 68 hydraulic oil.

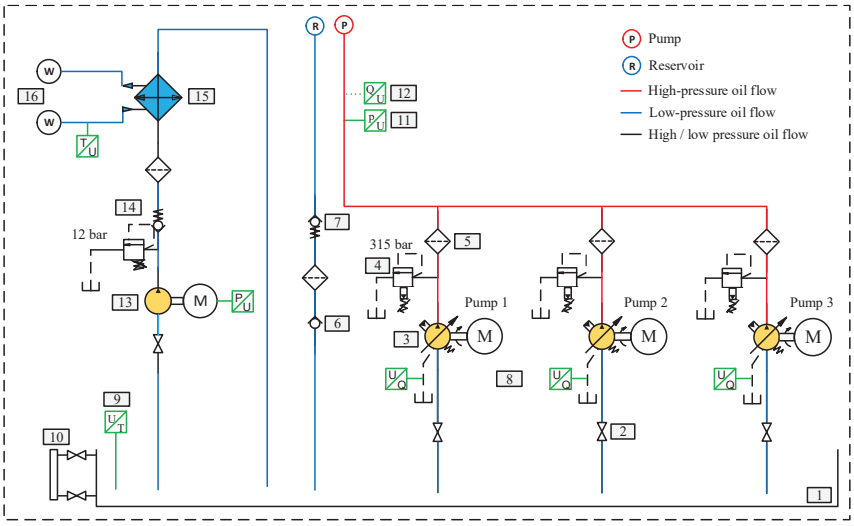

Figure 2 Simplified hydraulic schematic of the pump station and cooling units.

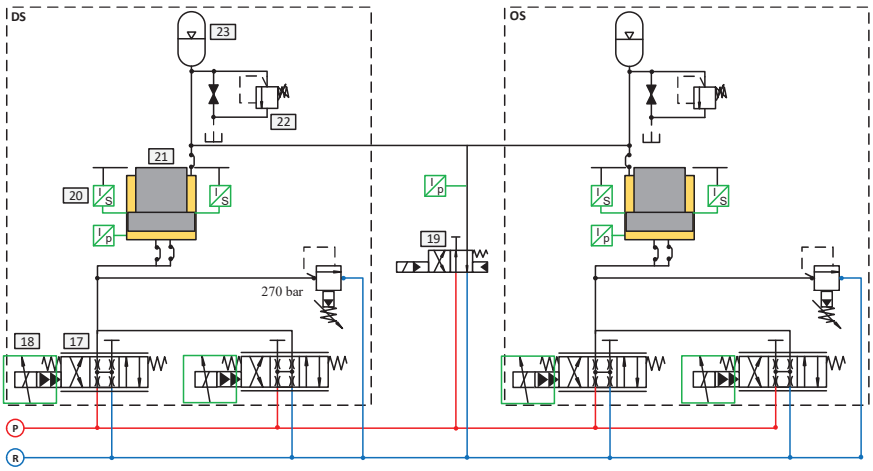

Figure 3 Simplified hydraulic schematic of the HGC cylinders unit.

3 Thermal Energy Modeling and Analysis Approach

Industrial hydraulic systems involve three key energy processes, as shown in Figure 7. First is the energy storage process, which typically occurs in hydraulic accumulators. Second is the energy loss process, happening throughout the system in components such as pumps, motors, cylinders,

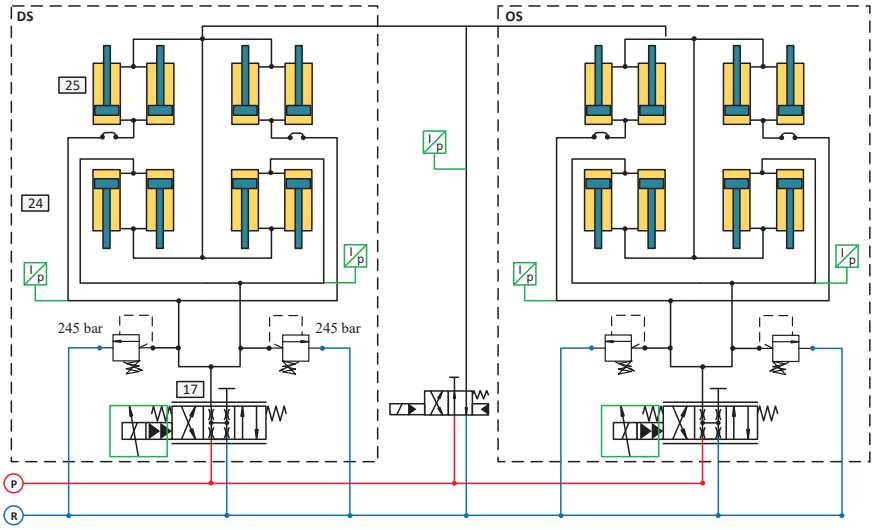

Figure 4 Simplified hydraulic schematic of the positive bending cylinders unit.

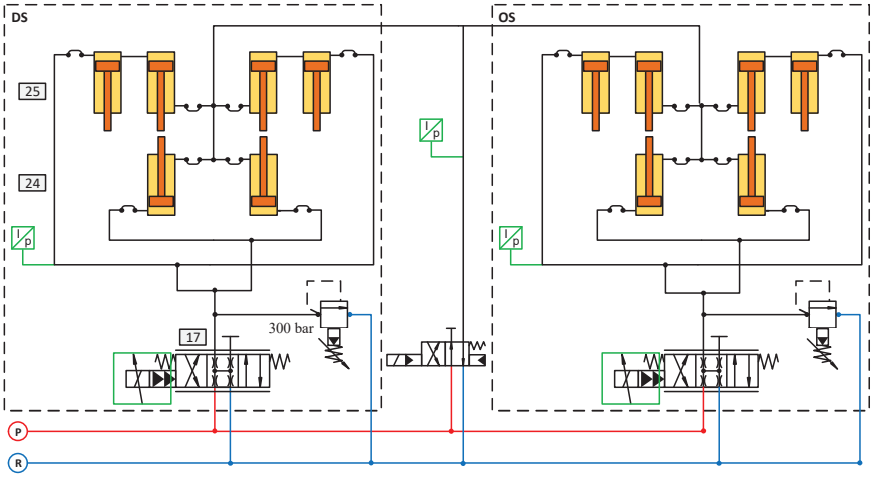

Figure 5 Simplified hydraulic schematic of the negative bending cylinders unit.

fittings, and valves. Third is the heat dissipation process, primarily taking place in the reservoir and cooling heat exchanger. These processes are interconnected and occur simultaneously, with the total energy of a hydraulic system being the sum of these three types of energy across all hydraulic components

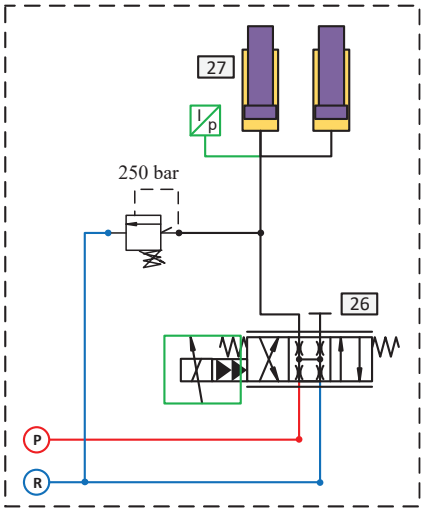

Figure 6 Simplified hydraulic schematic of the balancing cylinders unit.

Table 1 Components and measurement devices

No.	Designation	No.	Designation
1	Reservoir (2000 L − 3000 L)	15	Heat Exchanger (Cooler)
2	Butterfly valve with limit switch console	16	Source of Cooled Water
3	Pump (P 110 kW, 290 bar, 1500 RPM)	17	4/3-way Servo valve / Moog D661
4	Pressure relief valve (315 bar)	18	Valve opening signals
5	Hydraulic oil filter	19	4/2-way solenoid valve / Rexroth WEH
6	Free-floating check valve	20	Position Sensor
7	Spring loaded check valve	21	HGC Cylinder
8	Flow rate sensor	22	Safety and shut-off block
9	Temperature sensor	23	Bladder storage 10 dm3
10	Oil level sensor	24	hydraulic cylinders of lower work roll
11	Pressure sensor	25	hydraulic cylinders of upper work roll
12	Flow rate sensor (temporary)	26	4/3-way Servo valve / Moog D662
13	Pump (P 7.5 kW, 10 bar, 1500 RPM)	27	Balancing cylinders
14	Pressure relief valve (12 bar)		

In complex industrial hydraulic systems with multiple pumps, motors, cylinders, and other components, the local transient oil temperature T_l can vary by several degrees Celsius across different units. However, in most cases, precise knowledge of the transient oil temperature in each individual component is not essential for understanding the system's overall thermal dynamics.

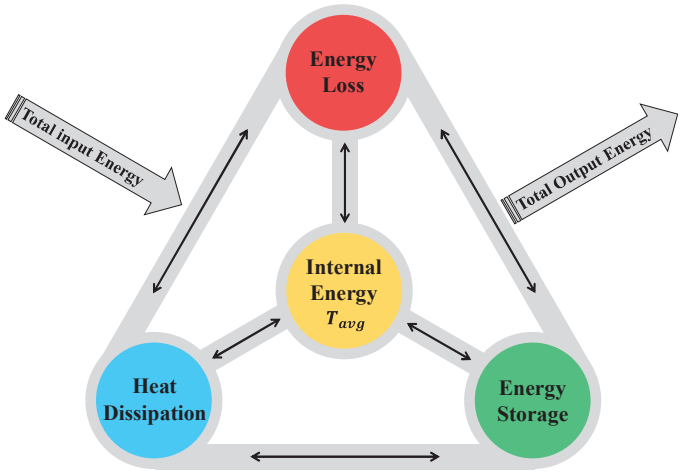

Figure 7 Coupled thermal processes in a hydraulic system [11].

In this study, the hydraulic system is assumed as a lumped-component system with a singular transient oil temperature. Consequently, all components or units within the industrial hydraulic system share the same transient temperature which is introduced as a new parameter, the average transient temperature T_{avg}.

This assumption simplifies the calculation of enthalpy and accelerates the modeling process without compromising the overall understanding of the hydraulic system's thermal behavior. Consequently, the average transient temperature approach effectively captures the internal energy dynamics within the hydraulic system, serving as a reliable indicator of its thermal state. In this context, the average temperature T_{avg} consistently falls between the two extreme oil temperatures, T_{max} and T_{min}, within the entire hydraulic system.

The net energy within hydraulic components is determined by summing the energy changes occurring within their control volumes, accounting for variations due to work or heat transfer. Inside the control volume of hydraulic components, energy can exist in various forms, including kinetic energy, potential energy, and internal thermal energy. When kinetic and potential energy contributions are neglected, the energy balance can be described exclusively in terms of thermal energy, as expressed by Eq. (1) [12].

$$m_{sys}\, c_p\, T_{avg} = \sum_{i=1}^{n} m_{c.i}\, c_{p.i}\, T_{l.i} \tag{1}$$

Notably, the total hydraulic oil mass within the system m_{Sys} is the sum of the oil masses contained in each hydraulic component m_c. Since the thermodynamic properties, such as specific heat capacity c_p, remain approximately uniform throughout the system, Equation (1) can be simplified to determine the average transient temperature of the hydraulic oil within the system, as shown in Equation (2):

$$T_{avg} = \frac{\sum_{i=1}^{n} m_{c.i}\, T_{l.i}}{m_{sys}} \tag{2}$$

Each individual component, with its local temperature, contributes to the overall average transient temperature of the system. The thermal contribution, or thermal share S_{therm}, of each local oil temperature to the entire hydraulic system is represented by Equation (3). It is defined as the ratio of the oil mass in a specific component to the total oil mass in the system, reflecting the weighting of each local temperature:

$$S_{therm} = \frac{m_c}{m_{sys}} \tag{3}$$

This derivation serves as the foundation for introducing the new parameter, T_{avg}. Therefore, it is essential to formulate the comprehensive differential equation for T_{avg}, employing lumped parameter assumptions to represent the system's thermal behavior. Figure 8 illustrates the block diagram of the thermal energy model, incorporating the average transient temperature.

3.1 Derivation of the Governing Equations

In formulating the governing equations for the current thermal model, it is essential to apply the conservation laws for both mass and energy. Based on the continuity equation for one-dimensional flow, the change in mass flow rate is represented by Equation (4), where the outlet mass flow rate is equal to the combined flow rates from the delivery and drain ports.

$$\frac{dm}{dt} = \dot{m}_{in} - \dot{m}_{de} - \dot{m}_{dr} \tag{4}$$

The mass of the liquid within the control volume of hydraulic component is given by $m = \rho V$. Differentiating the mass with respect to time allows the formulation of the density equation as follows:

$$\frac{d\rho}{dt} = \frac{1}{V}\left(\frac{dm}{dt} - \rho\frac{dV}{dt}\right) \tag{5}$$

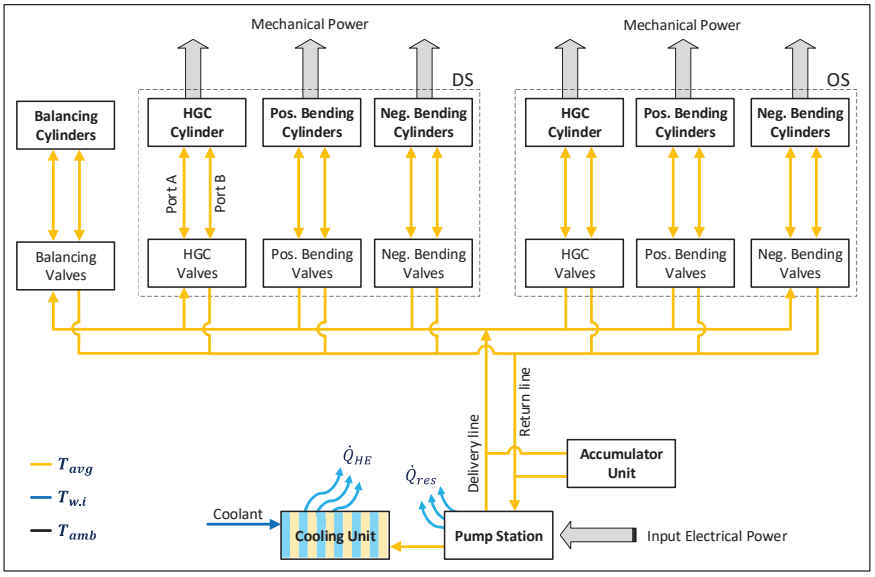

Figure 8 Block diagram of the thermal model for the industrial hydraulic system.

Since density is a thermodynamic property of the fluid, it is a function of both pressure and temperature, i.e., $\rho = f(p, T)$. By differentiating the density with respect to pressure and temperature, and then dividing by the change in time, the following relation is obtained:

$$\frac{dp}{dt} = \frac{1}{\left.\frac{\partial \rho}{\partial p}\right|_T} \left(\frac{d\rho}{dt} - \left.\frac{\partial \rho}{\partial T}\right|_p \frac{dT_{avg}}{dt} \right) \tag{6}$$

Utilizing the definition of fluid properties, specifically the isothermal bulk modulus (β_T) and the thermal expansion coefficient (α_p), and combining Equations (4) and (5), while substituting into Equation (6), results in:

$$\frac{dp}{dt} = \frac{\beta_T}{m} \left(\dot{m}_{in} - \dot{m}_{de} - \dot{m}_{dr} - \rho \frac{dV}{dt} \right) + \beta_T \alpha_P \frac{dT_{avg}}{dt} \tag{7}$$

The fundamental principle governing thermal variations within a hydraulic component or system is the first law of thermodynamics, as applied to a fluid volume undergoing a flow process. This is represented by Equation (8). For a detailed mathematical analysis, the ordinary differential

equation governing the energy of the hydraulic oil within a control volume (cv) of hydraulic component or system is derived as:

$$\dot{E}_{cv} + \dot{W}_{cv} = \dot{E}_f + \dot{W}_f + \frac{\delta W}{\delta t} - \frac{\delta Q}{\delta t} \tag{8}$$

Given that the enthalpy of a thermodynamic system is defined as the sum of its internal energy and the product of pressure and volume, the equation is reformulated in terms of enthalpy as:

$$\dot{H}_{cv} = \dot{H}_f + \frac{\delta W}{\delta t} - \frac{\delta Q}{\delta t} \tag{9}$$

The term $\delta W/\delta t$ represents the work done by the hydraulic component's shaft when Equation (9) is applied to an individual component. However, when the equation is applied to the entire hydraulic system, this term signifies the power loss. The minus sign for $\delta Q/\delta t$ accounts for the fact that, in industrial hydraulic systems, heat dissipation is more prevalent than heat absorption. The rate of enthalpy change over time can be expressed as:

$$\dot{H}_{cv} = \frac{d(mh)}{dt} = m\frac{\partial h}{\partial t}|_{cv} + h\frac{\partial m}{\partial t}|_{cv} \tag{10}$$

The specific enthalpy of hydraulic oil is a function of temperature and pressure, $h = f(p, T)$. Therefore, the time derivative of enthalpy can be expressed as:

$$\frac{\partial h}{\partial t}|_{cv} = c_p\frac{dT_{avg}}{dt} + (1 - \alpha_p T_{avg})\upsilon\frac{dp}{dt} \tag{11}$$

The change in enthalpy for the hydraulic component is given by the difference between the inlet and outlet ports (delivery and drain), as described by:

$$\dot{H}_f = \dot{m}_{in}\, h_{in} - \dot{m}_{de}\, h_{de} - \dot{m}_{dr}\, h_{dr} \tag{12}$$

The energy equation, Equation (9), can be reformulated in terms of the time derivatives of temperature. Assuming that h_{de} equals the specific enthalpy of the control volume, and by combining Equations (4), (10), (11), and (12), and substituting them into Equation (9), the following expression is obtained:

$$\begin{aligned}\frac{dT_{avg}}{dt} = \frac{1}{mc_p}\left(\dot{m}_{in}\,(h_{in} - h) - \dot{m}_{dr}\,(h_{dr} - h) + \frac{\delta W}{\delta t} - \frac{\delta Q}{\delta t}\right) \\ + \frac{(\alpha_p T_{avg} - 1)}{\rho c_p}\,\frac{dp}{dt}\end{aligned} \tag{13}$$

Equations (7) and (13) represent the lumped parameter models for the conservation of mass and energy. It is evident that these two equations are inherently coupled, meaning that rapid pressure transients will induce corresponding rapid temperature transients, and vice versa. For simplification, the following five symbols are introduced: C_1, C_2, and C_3 for the continuity equation, and E_1 and E_1 for the energy equation.

$$C_1 = \frac{\beta_T}{m}\left(\dot{m}_{in} - \dot{m}_{de} - \dot{m}_{dr}\right) \tag{14}$$

$$C_2 = \frac{\beta_T}{V} \tag{15}$$

$$C_3 = \beta_T \alpha_p \tag{16}$$

$$E_1 = \frac{1}{mC_p}\left(\dot{m}_{in}\left(h_{in} - h\right) - \dot{m}_{dr}\left(h_{dr} - h\right) + \frac{\delta W}{\delta t} - \frac{\delta Q}{\delta t}\right) \tag{17}$$

$$E_2 = \frac{\left(\alpha_p T_{avg} - 1\right)}{\rho C_p} \tag{18}$$

These two differential Equations (7) and (13) can be decoupled by solving for each derivative independently, yielding the following results:

$$\frac{dT_{avg}}{dt} = \frac{\left(C_1 + C_2 \frac{dV}{dt}\right) E_2 + \ E_1}{1 - C_3 \ E_2} \tag{19}$$

Equation (19) serves as a general formula applicable to both individual hydraulic components and the entire hydraulic system. It is an explicit differential equation, providing various options for numerical integration. For the modelling implementation, however, the Explicit Runge-Kutta method was utilized.

3.2 Flow Rate Calculations

In this study, we utilize two distinct signals to estimate the flow rate during the extension and retraction strokes of hydraulic cylinders, mitigating the high costs associated with permanent flow rate sensors. These signals include the displacement (position) sensor and the servo valve opening signal (command signal). Using these sensors and signals, the oil flow rate can be calculated as follows:

- For position sensors

$$\frac{dV}{dt} = A\frac{ds}{dt} \tag{20}$$

- For valve opening signals

$$\frac{dV}{dt} = \begin{cases} Q_{null.leak} & if\ y = 0 \\ y\ k_V\ \sqrt{\triangle p} - Q_{pilot.leak} & if\ y > 0 \end{cases} \tag{21}$$

During the flow rate calculation, Equations (20) and (21) are applied to both ports A and B. The flow rate for the extension stroke is determined from port A, while the flow rate for the retraction stroke is determined from port B.

3.3 Power Loss Calculations

The power losses due to mechanical work entering and leaving the hydraulic system are described as follows:

$$\frac{\delta W}{\delta t} = +\sum \dot{W}_{pp} - \sum \dot{W}_{acts} \tag{22}$$

Given that both scenarios occur simultaneously, plus and minus signs are used to represent the work done. In the first case, where work is done on the system by a hydraulic pump, a positive sign is used. Conversely, in the second case, where work is performed by the system through a hydraulic motor or cylinder, a negative sign is applied.

To generalize the formula for calculating the time derivative of mechanical work for both a hydraulic pump and motor, Equation (23) is used, where K $= 1$ for a pump and K $= -1$ for a motor. The overall efficiency η_o of a hydraulic machine is defined as the ratio of output power to input power and can either be obtained from manufacturer specifications or determined empirically.

$$\dot{W} = \left(\frac{K}{\eta_o}\right)^K \dot{H}_f \tag{23}$$

Assuming $\dot{m}_i = \dot{m}_{de} + \dot{m}_{dr}$, we can rewrite Equation (12) to determine the hydraulic power for both the hydraulic pump and the hydraulic motor as follows:

$$\dot{H}_f = \dot{m}_{de}\ (h_{de} - h_i) + \dot{m}_{dr}\ (h_{dr} - h_i) \tag{24}$$

The change in enthalpy, depending on the definition, is a function of temperature and pressure, expressed as $dh = f(\overline{T}, dT, dp)$. By applying Equation (11) to two ports and ignoring the time derivative, we arrive at the following expressions for the pump and motor:

$$\begin{aligned} \dot{H}_f = {} & \dot{V}_{de}\rho\bar{c}_p(T_{de} - T_i) + \dot{V}_{de}(1 - \alpha_p\overline{T})(p_{de} - p_i) \\ & + \dot{V}_{dr}\rho\bar{c}_p(T_{dr} - T_i) + \dot{V}_{dr}(1 - \alpha_p\ \overline{T})(p_{dr} - p_i) \end{aligned} \tag{25}$$

A similar procedure can be applied to the hydraulic cylinder, but with two distinct ports. Port A refers to the piston side, while port B corresponds to the rod side.

$$\dot{H}_f = \dot{H}_A - \dot{H}_B \tag{26}$$

$$\dot{H}_f = \dot{V}_A \rho c_p dT_A + (1 - \alpha_p T_A)\dot{V}_A p_A - \dot{V}_B \rho c_p dT_B - (1 - \alpha_p T_B)\dot{V}_B p_A \tag{27}$$

A key assumption is that the transient temperature of the hydraulic oil is uniform throughout the system, represented by T_{avg}. As a result, temperature differences across all ports of the hydraulic components – including the inlet, outlet, piston, and rod – are neglected during the calculation of enthalpies.

Consequently, the change in specific enthalpy becomes a function of the average transient temperature and the pressure drop, $dh = f(T_{avg}, dp)$. Applying this to Equations (25) and (27), and then substituting the results into Equation (23), leads to the derivation of Equation (28) for calculating the mechanical power of the hydraulic pump or motor, and Equation (29) for the mechanical power of the hydraulic cylinder.

$$\dot{W} = \left(\frac{K}{\eta_o}\right)^K ((1 - \alpha_p T_{avg})(\dot{V}_{de}(p_{de} - p_i) + \dot{V}_{dr}(p_{dr} - p_i))) \tag{28}$$

$$\dot{W} = \eta_o(\rho c_p dT_{avg}(\dot{V}_A - \dot{V}_B) + (1 - \alpha_p\, T_{avg})|(\dot{V}_A p_A - \dot{V}_B p_B)|) \tag{29}$$

We use the temperature change (dT_{avg}) because temperature is an intrinsic property of the oil. Consequently enthalpy calculations require a relative temperature change rather than the absolute temperature. To ensure a positive value for both extending and retracting strokes, the power term $(\dot{V}_A p_A - \dot{V}_B p_B)$ is enclosed in absolute value brackets.

3.4 Mathematical Model for Heat Dissipation

In industrial hydraulic systems, the temperature of hydraulic oil is generally managed through two methods: passive and active heat dissipation. Passive dissipation occurs via the surfaces of all hydraulic components, while active dissipation utilizes heat exchangers. Estimating the heat loss from all component surfaces is difficult due to the variable operating conditions and numerous external factors related to installation. Additionally, heat dissipation from component surfaces is relatively small compared to that from the reservoir and the heat exchanger.

To simplify the calculation of total heat dissipation, this research focuses solely on the reservoir (res) and the heat exchanger (HE), specifically a single-pass counter-flow double-wall plate heat exchanger, as illustrated in Figure 9.

The governing heat dissipation for the industrial hydraulic system application of this study is:

$$\frac{\delta Q}{\delta t} = \frac{\delta Q_{res}}{\delta t} + \frac{\delta Q_{HE}}{\delta t} \tag{30}$$

For the reservoir, we assumed that the interior air, ambient temperature, and each wall could be treated as lumped parameters. The total heat dissipation capacity of a hydraulic reservoir is comprised of the heat dissipation through the "oil contact part" and the "air contact part", see Figure 9, (a). Therefore, two thermal resistances – Figure 10 – have to be considered during the analysis.

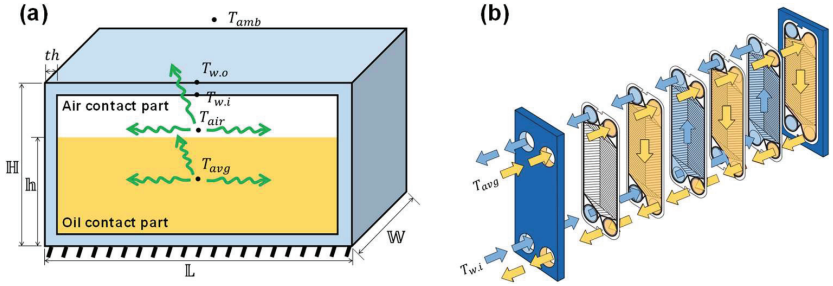

Figure 9 Schematic of heat dissipation (a) reservoir (b) double wall plate heat exchanger.

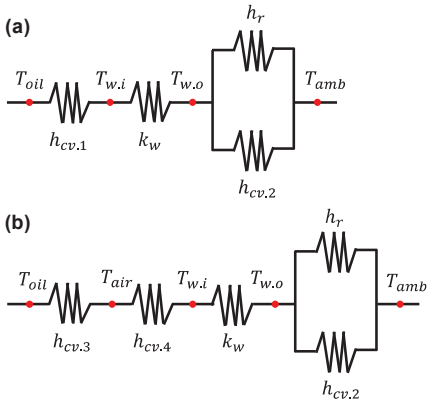

Figure 10 Schematic of thermal resistance of (a) oil contact part (b) air contact part.

Equation (31) is to calculate heat transfer to ambient in terms of temperature and thermal resistance.

$$\dot{Q}_{res} = (T_{avg} - T_{amb}) \left(\frac{R_{t.1} + R_{t.2}}{R_{t.1} R_{t.2}} \right) \tag{31}$$

The total equivalent thermal resistance between the hydraulic oil and ambient air through the wall, $R_{t.1}$ as follows:

$$R_{t.1} = \frac{1}{h_{cv.1} A_{oil.w}} + \frac{th}{k_w A_{oil.w}} + \frac{\frac{1}{h_{cv.2} A_{oil.w}} \frac{1}{h_r A_{oil.w}}}{\frac{1}{h_{cv.2} A_{oil.w}} + \frac{1}{h_r A_{oil.w}}} \tag{32}$$

While the total equivalent thermal resistance between the hydraulic oil and ambient air through the interior air, $R_{t.2}$ is:

$$R_{t.2} = \frac{1}{h_{cv.3} A_{oil.air}} + \frac{1}{h_{cv.4} A_{air.w}} + \frac{th}{k_w A_{air.w}} + \frac{\frac{1}{h_{cv.2} A_{air.w}} \frac{1}{h_r A_{air.w}}}{\frac{1}{h_{cv.2} A_{air.w}} + \frac{1}{h_r A_{air.w}}} \tag{33}$$

The radiative heat transfer coefficient is given by:

$$h_r = \sigma \times \epsilon \times ({T_{avg}}^2 + {T_{amb}}^2) \times (T_{avg} + T_{amb}) \tag{34}$$

The contact areas between the oil and inner wall, oil and interior air, as well as the interior air and inner wall, are calculated using the following equations:

$$A_{oil.w} = 2(L + W)(h) \tag{35}$$

$$A_{oil.air} = L * W \tag{36}$$

$$A_{air.w} = 2(L + W)(H - h) + L * W \tag{37}$$

Heat exchangers typically operate with minimal variations in their operating conditions over extended periods, allowing them to be modelled as steady-flow devices. The overall energy balance at the inlet ports of the hydraulic oil and coolant can be analyzed using the effectiveness-NTU method as follows:

$$\dot{Q}_{HE} = \varepsilon \, \dot{Q}_{HE.max} \tag{38}$$

$$\dot{Q}_{HE.max} = C_{min}(T_{avg} - T_{c.i}) \tag{39}$$

Where C_{min} is the smaller of $C_h = \dot{m}_{oil} c_{p.oil}$ and $C_c = \dot{m}_w c_{p.w}$. However, it requires knowledge of the heat exchanger effectiveness ε, which can

be obtained from the mathematical relations, Equation (40). Alternative way to determine effectiveness is through experimentation via calculate actual heat transfer.

$$\varepsilon = \frac{e^{[(1-C_r)NTU_{min}]} - 1}{e^{[(1-C_r)NTU_{min}]} - C_r} \tag{40}$$

Where:

$$C_r = \frac{C_{min}}{C_{max}} \tag{41}$$

$$NTU = \frac{UA_s}{C_{min}} \tag{42}$$

3.5 Hydraulic Oil Specifications

The majority of currently used hydraulic oils in industrial hydraulic systems are derived from mineral oil, chosen primarily for their cost-effective performance [13]. Hydraulic oils describe the transfer of energy and signals through fluids; in this transmission process, power is transferred to drive, control and move [14]. When selecting mineral oil, it is essential to consider specific system requirements and operating conditions, including temperature, pressure, load, speed, and equipment type. The density and viscosity of hydraulic oil play a pivotal role in pump efficiency, contamination control, pressure loss, leakage prevention, lubrication, and addressing challenges like oil cavitation. Additionally, hydraulic oil specifications, including isobaric thermal expansion and isothermal compressibility, are vital for maintaining overall system performance efficiency and temperature management [15–17].

In this research we considered the variation of hydraulic oil specifications ρ, μ, β_T, and α_p using the PINN model, Figure 11, created by Al-Issa and Weber [18]. This innovative model, based on the laws of physics, enhances our thermal simulation by allowing it to predict four of oil properties in one correlation model.

However, we made some improvements to the PINN model to meet our need for HLP 68. The main improvements illustrated in Table 2 have been done on the model is using a different training data, new activation function (softmax), Equation (43), increased the predicted data to be 25000 and new value of Decay rate is 10^{-7}.

$$\mathcal{S}(\overrightarrow{\mathcal{Z}})_i = \frac{e^{\mathcal{Z}_i}}{\sum_{j=1}^{n} e^{\mathcal{Z}_j}} \tag{43}$$

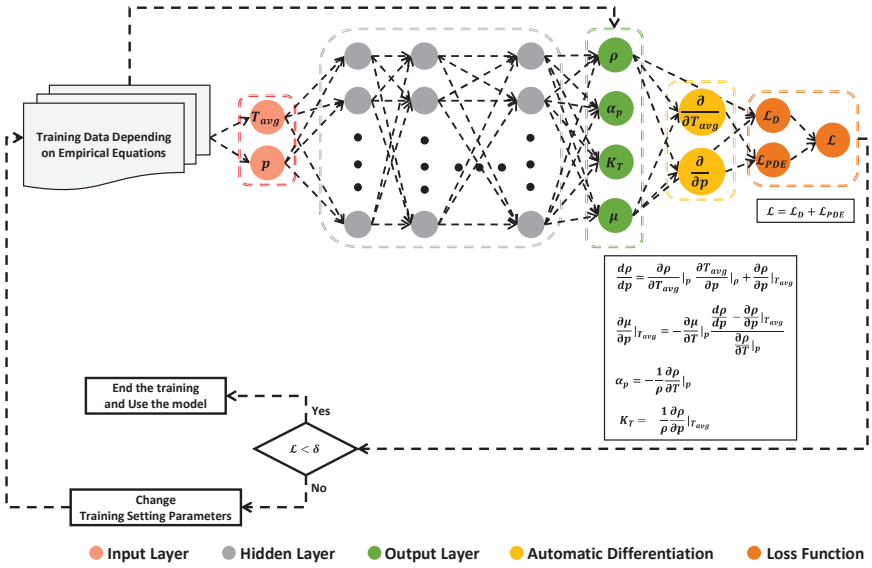

Figure 11 The schematic diagram of the current PINN model.

Table 2 Optimum parameters for the PINN models, HLP 68

Setting Parameter	Value
No of hidden layer	2
No of neurons per layer	420
No of epoch	500
Learning rate	0.01
Decay rate	10^{-7}
Empirical training data	30
Predicted data	25,000
Mini batch	100
Activation Function	Softmax
Optimizer	ADAM

In the PINN model, we depend on two parameters; average transient temperature and main pressure of hydraulic oil to determine density, viscosity, thermal expansion and composability. Figure 12 is displayed randomly chosen examples of plotting corresponding density, viscosity, expansion and compressibility curves at each temperature point for pressure values of (0, 100, 200, and 300) bar.

The isobar specific heat capacity $c_{p.oil}$ for the HLP 68 is given in Equation (44) [19] while the thermal conductivity k_{oil} can be calculated according

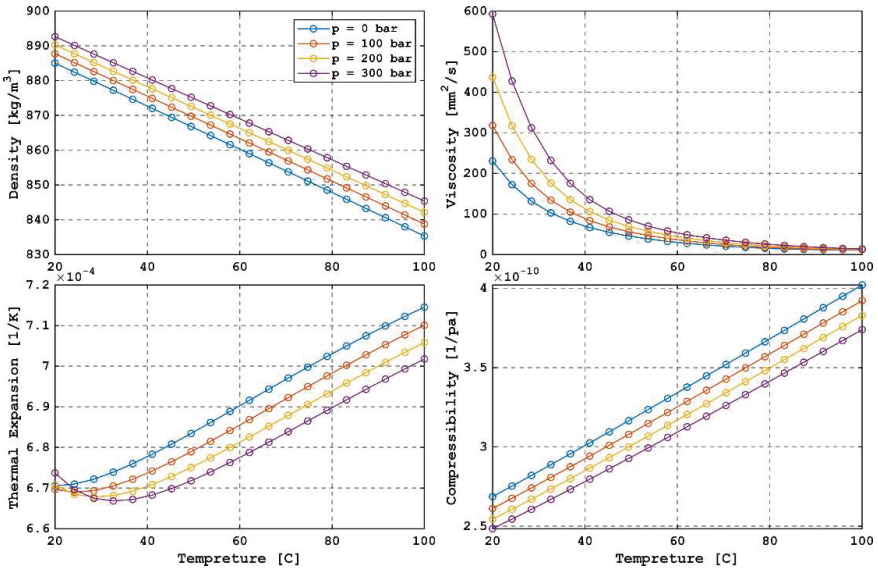

Figure 12 Specifications of hydraulic oil HLP 68 using PINN model.

to Equation (45) [19]:

$$c_{p.oil} = \lambda_1 + \lambda_2(T_{avg}) \tag{44}$$

With

$$\lambda_1 = 915.8\ J/kg.K$$
$$\lambda_2 = 3.8\ J/kg.K$$

$$k_{oil} = \lambda_3 - \lambda_4\ (T_{avg} - 298.15) \tag{45}$$

With

$$\lambda_3 = 0.15\ W/m.K$$
$$\lambda_4 = 1.4 \times 10^{-4}\ 1/m.K^2$$

4 Initial Temperature Selection

Two distinct thermal conditions must be considered: overheating and healthy. The healthy condition ranges from the actual operating temperature, T_{act}, up to the maximum permissible temperature, T_{per}. In contrast, the overheating

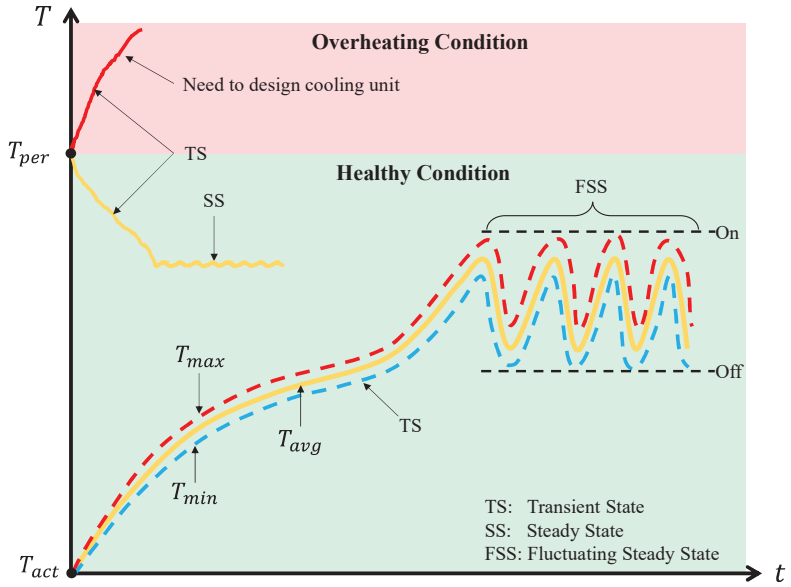

Figure 13 Thermal behavior of hydraulic oil in an industrial hydraulic system.

condition occurs when temperatures exceed T_{per}. Typically, when hydraulic systems are initiated, the thermal behavior of the hydraulic oil starts in a transient state (TS) within the healthy condition, which may transition to a steady state (SS) or remain in the transient state, depending on the operating conditions. Achieving precise thermal equilibrium – where heat dissipation equals energy losses – is difficult for many hydraulic systems. As a result, the internal energy of the system often increases as long as the heat dissipation from the reservoir remains insufficient.

To mitigate this, cooling units are used. These units activate (On) when the hydraulic oil reaches predefined temperature thresholds and deactivate (Off) once the oil cools to specific levels. This causes temperature fluctuations in the hydraulic oil, referred to as Fluctuating Steady State (FSS). Therefore, our thermal modeling approach can begin from one of two possible paths, as illustrated in Figure 13 and detailed below:

1 – Direct Thermal Modeling

In cases where no external cooling unit is used and heat dissipation depends solely on the reservoir, designers focus on testing the reservoir's capability to keep the oil within its designated temperature range and prevent overheating.

Direct Thermal Modeling provides a quick and efficient method for assessing the thermal condition of the hydraulic system by comparing it to the maximum permissible temperature of the hydraulic oil. This approach begins by setting the initial temperature of the hydraulic oil, as follows:

$$T_{avg}|_{t=0} = T_{per}$$

If the internal energy of the hydraulic system continues to rise at this temperature, it indicates an overheating condition, necessitating the design of a cooling unit. Otherwise, the system should eventually stabilize at a Steady State (SS), signifying efficient operation without the need for a cooling unit.

2 – Standard Thermal Modeling

Whether or not a cooling unit is present, it is advisable to use a Standard Thermal Modelling approach to estimate the thermal behavior of the hydraulic oil. This method is effective for predicting the oil temperature after a specific duration or calculating the time required for the oil to reach a certain temperature.

In this approach, the initial value of T_{avg} is assumed to be the actual hydraulic oil temperature in the reservoir, from which the modelling begins, as shown below:

$$T_{avg}|_{t=0} = T_{act}$$

5 Results and Discussion

All input data relies solely on three measurements: displacement sensors, pressure, and valve opening signals. The duty cycle of p, dx and y is used for all cylinders and servo valves. Temperature measurements are utilized exclusively for validation purposes. Figure 14 provides a visual guide to the step-by-step implementation process of the governing equation, Equation (19), starting from the experimental data until the output results; flow rate, mechanical power, heat dissipation, oil temperature, oil specifications and normalized error.

From the displacement sensor readings and the servo valve opening signals, we calculated the flow rates for the 4 hydraulic cylinders units. The main flow rate from the pumps was measured over a specific time period to verify and compare with the calculated flow rate as is depicted in the Figure 15. It is evident from the measurement data that there are anomalous

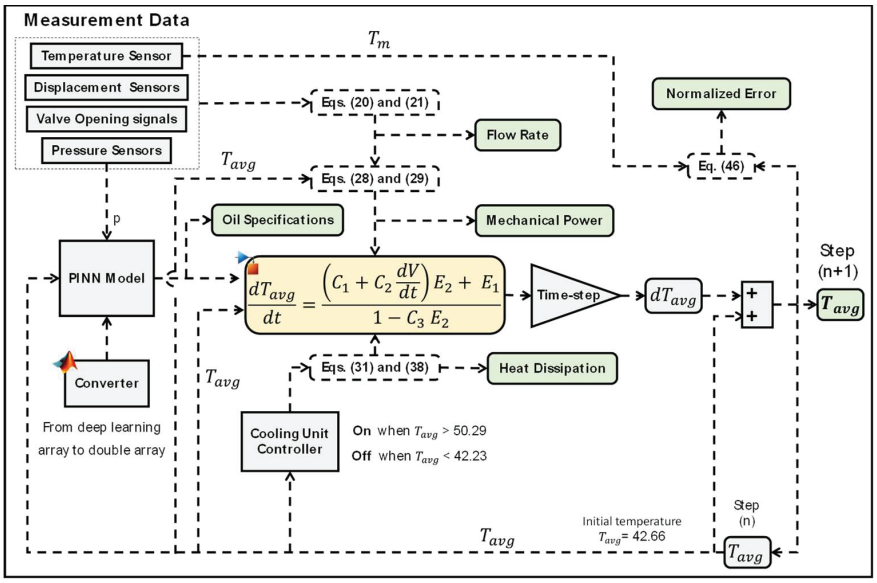

Figure 14 Simplified scheme of the implementation process.

peaks that do not correspond to the predicted values. These deviations are likely a result of the fast dynamic cylinder movements.

In this system, the primary focus is on the energy consumption of the hydraulic cylinders (HGC, positive bending, negative bending and balancing), as all mechanical work is derived from them; thus, the accumulator unit was not analyzed. Using experimental duty cycle data obtained from pressure measurements and calculated flow rates, the mechanical power produced by all cylinders (HGC, positive bending, negative bending and balancing) within the hydraulic system was computed according to Equation (29). Figure 16 presents an example of the hydraulic power distribution for each unit.

For determining heat dissipation, as shown in Figure 17, the heat dissipated from the reservoir fluctuates over time, ranging from about $0.6\ kW$ to $1.1\ kW$. Regarding the cooling unit, the oil flow rate circulating through it is $150.7\ l/min$, while the water flow rate is $265\ l/min$. As a result, the minimum heat capacity rate, C_{min}, corresponds to the oil and is calculated to be $5\ Wm^3/kg.K$, which is then applied in Equation (39). Consequently, Equation (38) is also applied, leading to the conclusion that the cooling unit accounts for approximately 98% of the total heat dissipation.

The normal operating oil temperature is influenced by ambient temperature, system pressure, and other factors. For axial variable piston pump units,

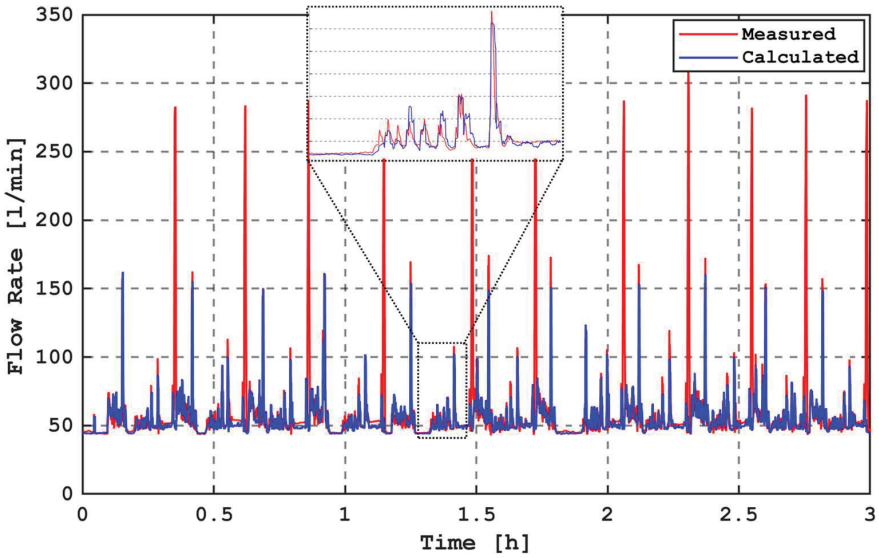

Figure 15 Measured and calculated flow rate.

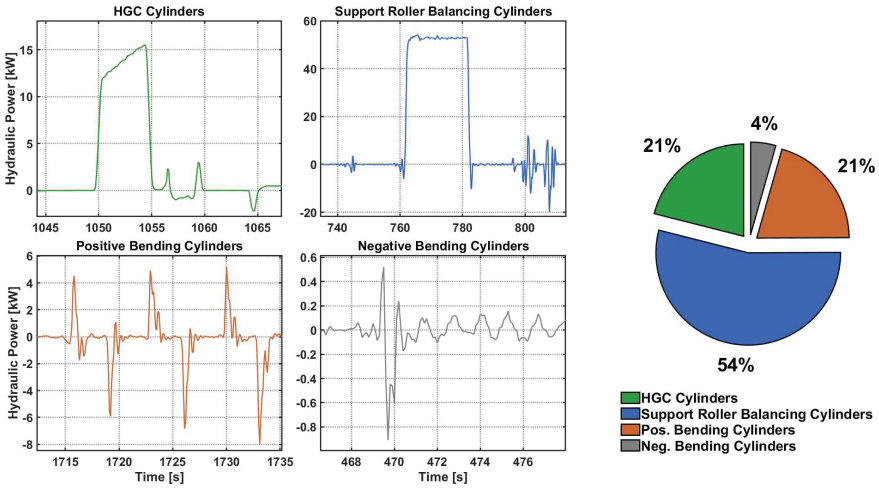

Figure 16 Hydraulic power of all hydraulic cylinder units.

depending on their construction and operating conditions, the valid viscosity range for continuous operation is between 400 mm^2/s and 10 mm^2/s and for optimal operation is between 16 mm^2/s and 36 mm^2/s [20]. Therefore, for hydraulic oil type HLP 68, the corresponding temperature range at

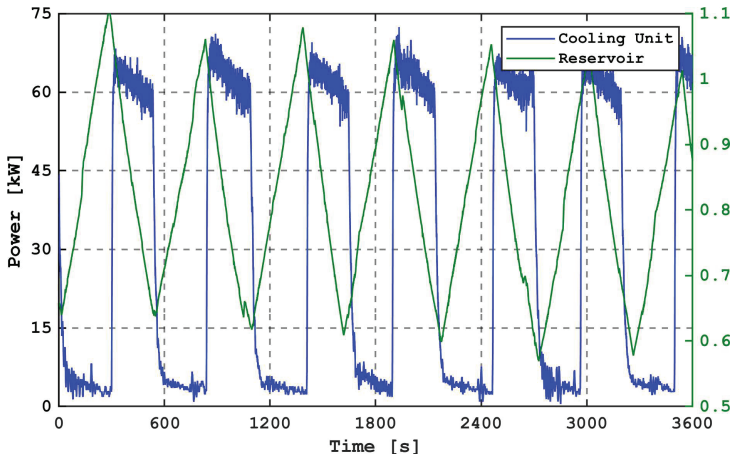

Figure 17 Heat dissipation.

maximum pressure in the system ($\approx$290 bar) is from $+11$°C to $+95$°C for continuous operation and from $+54$°C to $+78$°C for optimal operation.

However, the average transient temperature of mineral-based hydraulic oils should not exceed $50-60$°C in stationary hydraulic systems and $80-90$°C in mobile hydraulic systems [14].

When implementing the direct thermal modelling approach to assess the need for a cooling unit, an initial temperature of 60°C should be used. As shown in Figure 18, the heat dissipation from the hydraulic reservoir is insufficient, as indicated by the continuous rise in average temperature after 60 seconds.

Thus, the standard thermal modelling method can now be applied. While the average transient temperature of the oil (which represents the internal energy of the entire hydraulic system) is a more comprehensive metric, it is not feasible to measure directly. The average transient temperature is influenced by localized heat generation, fluid motion, and heat transfer dynamics, which vary throughout the system's components. Installing sensors throughout the entire hydraulic circuit to measure these variations would be impractical.

For validation purposes, we chose to compare the simulated average transient temperature with the oil temperature in the reservoir, where 85% of the oil volume is contained and relatively well-mixed with the return flow. The temperature sensor, Sensor 9, installed in the bottom of the reservoir, was selected as a practical and suitable location for temperature

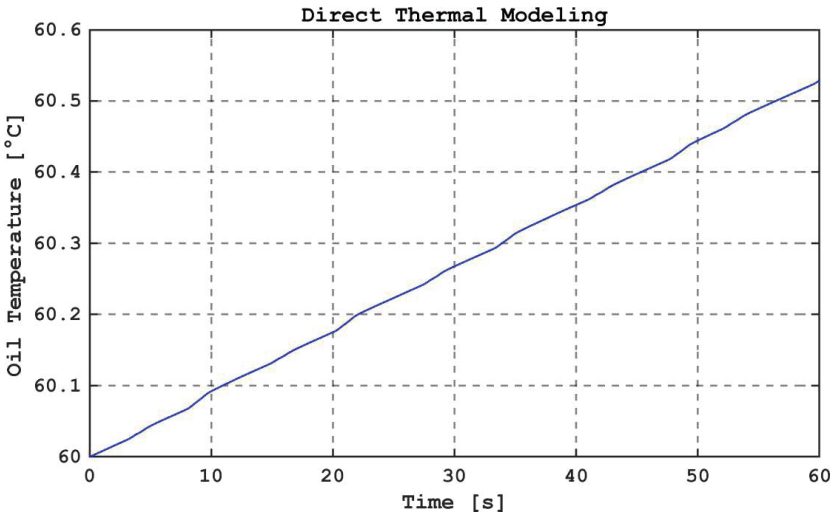

Figure 18 Simulated oil temperatures using direct thermal modelling path.

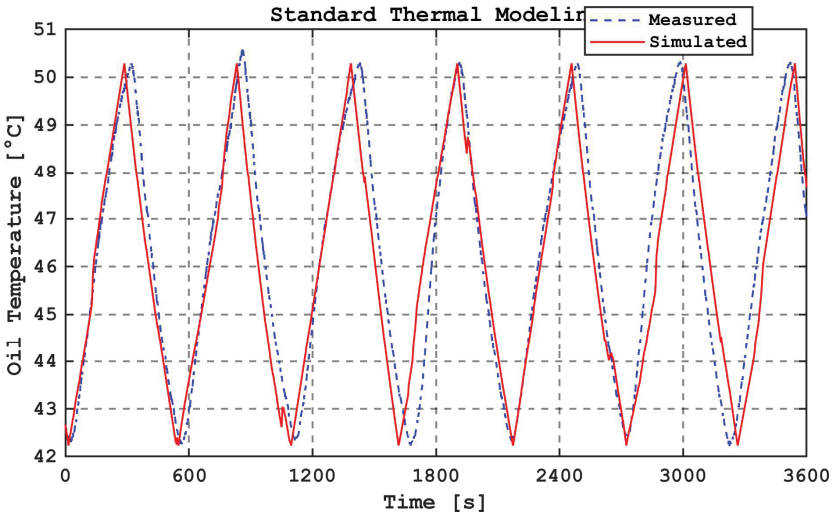

Figure 19 Measured and simulated oil temperatures for one hour.

measurement. Initial temperature for starting the modelling is got from the measurement which is $42.66°$C. Figure 19 presents the comparison between the measured and simulated temperatures, demonstrating a close match, with a final temperature difference of approximately $0.62°$C.

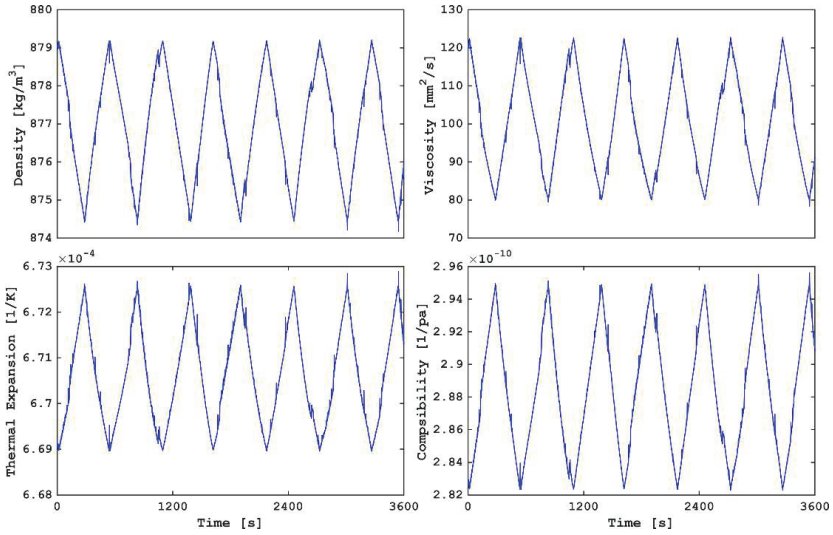

Figure 20 Specifications of hydraulic oil HLP 68 during thermal modeling process.

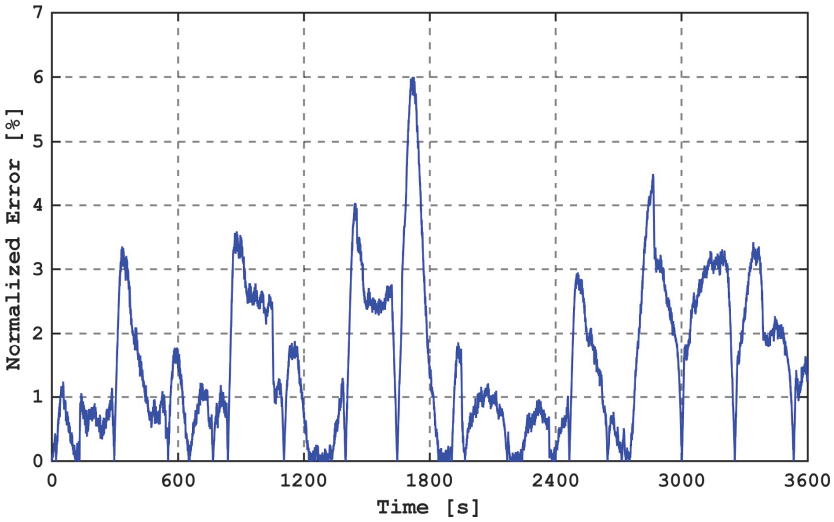

Figure 21 Normalized error of the thermal modeling.

The specifications of hydraulic oil during normal operation were modeled using the PINN model, as shown in Figure 20. The specifications fluctuate between two values due to changes in oil temperature, while the observed peaks are attributed to abrupt changes in pressure. The normalized error

Table 3 Time-step cases for thermal modelling

Case	Time-step [s]	Elapsed Time [s]	Time Ratio	Average Error [%]
1	1×10^{-3}	180.2	0.05	1.92
2	1×10^{-4}	2398.4	0.66	

Table 4 Required parameters for current thermal modeling

Parameter	Value	Unit	Parameter	Value	Unit
$C_{p.w}$	4180 [12]	$J/kg.K$	$\mathbb{L}$	2.068	m
$h_{cv.1}$	500 [21]	$W/m^2.K$	$\mathbb{W}$	1.168	m
$h_{cv.2}$	8.5 [22]	$W/m^2.K$	$\mathbb{H}$	1.055	m
$h_{cv.3}$	7 [21]	$W/m^2.K$	h	0.8 – 0.84[1]	m
$h_{cv.4}$	7 [21]	$W/m^2.K$	$Q_{null.leak}$	5.4 [23]	l/min
h_r	0.69 – 0.74[2]	$W/m^2.K$	$Q_{null.pilot}$	2.6 [23]	l/min
k_{wall}	15 [12]	$W/m.K$	ρ_w	998	kg/m^3
k_V	10.75 [23]	$l/(min.\sqrt{bar})$	ε	$0.35 - 0.43$[1]	–
ε	0.35 [24]	–			

[1]Measured based on oil level sensor.

[2]Calculated using experimental measurements.

of the proposed thermal modeling and analysis method is calculated using Equation (46), by comparing the experimentally measured hydraulic oil temperatures with the simulated values. Refer to Figure 21 for details.

$$E_n = \frac{\sqrt{\sum_{n=1}^{N} |T_{avg} - T_m|^2}}{\sqrt{\sum_{n=1}^{N} |T_m|^2}} \tag{46}$$

Finally, the simulation was run in MATLAB Simulink for two time-steps: 10^{-3} s and 10^{-4} s, using the ODE45 solver on a PC with an Intel Core i5 processor and 32 GB of RAM. Table 3 shows the elapsed time, time ratios between simulated and real time, and the average normalized error. The time ratios confirm that the proposed approach managed to speed up the modeling process to below real-time. The parameter values used in the modeling are found in Table 4.

6 Conclusion

This study presents a comprehensive thermal approach designed for industrial hydraulic system applications, employing new parameter average transient temperature of the hydraulic oil for modelling and analysis. This approach

was developed, demonstrated, and experimentally validated. Results indicated that ignoring oil temperature differences at hydraulic component ports when calculating enthalpies does not significantly affect the main trend of the oil's transient temperature within the hydraulic system. Notably, this reduces the need for temperature parameters during modeling, which in turn decreases modeling time less than experimental periods.

PINN model helps the thermal model to predict four thermophysical properties just in one correlation model. Future endeavors for researchers interested in this field of neural networks could entail exploring the additional oil properties such as enthalpy, isobaric specific heat capacity, thermal conductivity, and so on.

The maximum normalized error presented is 6 % and does not indicate any deficiencies in the methodology but arises from two factors. First, accurately estimating power loss and heat dissipation is inherently challenging due to their intricate dependence on the operational conditions of the hydraulic pumps and cylinders, as well as various external variables associated with installation conditions. Second, the oil temperature sensor used for validation does not necessarily represent the exact average transient temperature of oil in the hydraulic system, as it is the scope of our thermal model. Therefore, upon more precise calculations for power loss and heat dissipation, the error is expected to diminish accordingly.

Nomenclature

A	Area	m^2
c_p	Specific heat capacity	$J/kg.K$
C_1	Parameters of continuity equation	$m^2/N.s$
C_2	Parameters of continuity equation	$1/N.m$
C_3	Parameters of continuity equation	$m^2/N.K$
E	Total energy	J
E_n	Normalized error	$\%$
E_1	Parameters of energy equation	K/s
E_2	Parameters of energy equation	J/m^3K
H, h	Heat and specific enthalpy respectively	J
$\mathbb{H}$, h	Height of reservoir and oil respectively	m
$h_{cv.1}$	Convective heat transfer coefficient of oil	W/m^2K
$h_{cv.2}$	Convective heat transfer coefficient of ambient	W/m^2K
$h_{cv.3}$	Convective heat transfer coefficient of oil surface	W/m^2K
$h_{cv.4}$	Convective heat transfer coefficient of interior air	W/m^2K

h_r	Radiative heat transfer coefficient	W/m^2K
K	Constant	$-$
k_V	Flow rate coefficient	$l/(min.\sqrt{bar})$
k	Thermal conductivity	$W/m\ K$
$\mathbb{L}$	Length of the reservoir	m
m	Mass	kg
n	Counting variable or index	$-$
N	final index	$-$
p	Pressure	N/m^2
Q	Heat transfer	J
R_t	Thermal resistance	K/W
s	Displacement	m
S_{therm}	Thermal share	$-$
t	Time	s
T	Temperature	K
th	thickness	m
V	Volume	m^3
ν	specific volume	m^3/kg
W	Work	J
$\mathbb{W}$	Width of the reservoir	m
y	Servo valve opening	$\%$
$\overrightarrow{\mathcal{Z}}$	Input vector of PINN	$-$
β_T	Bulk modulus	m^2/N
α_p	Thermal expansion coefficient	$1/K$
ε, ϵ	Effectiveness, Emissivity of stainless steel	$-$
ρ	Density	kg/m^3
μ	kinematic viscosity	mm^2/s
δ	Softmax function	$-$
$e^{\mathcal{Z}_i}$	Standard exponential function for input vector	$-$
$e^{\mathcal{Z}_i}$	Standard exponential function for output vector	$-$

Subscripts

A	Chamber of piston side	i	Inlet
B	Chamber of rod side	l	Local
Air	Air	m	Measured
$acts$	Actuators	max	Maximum
amb	ambient	min	minimum
avg	Average	o	outlet

c	Component	oil	Hydraulic oil
co	coolant	per	permissible
cv	Control volume	pp	Pumps
de	Delivery	res	Reservoir
dr	drain	s	simulated
f	Flow	sys	Hydraulic system
HE	Heat exchanger	w	Wall

Superscripts

.	Time derivative
$-$	Mean value
$\rightarrow$	Vector

Abbreviations

DCV	Directional control valve
DS	Drive side
HGC	Hydraulic Gap Control
OS	Operator side
PINN	Physics informed neural network

References

[1] R. M. Harris, 'The modelling and simulation of temperature effects in hydraulic systems', PhD Thesis, University of Bath, 1990.

[2] J. A. Sidders, D. G. Tilley, and P. J. Chappie, 'Thermal-Hydraulic Performance Prediction in Fluid Power Systems', *Proceedings of the Institution of Mechanical Engineers, Part I: Journal of Systems and Control Engineering*, vol. 210, no. 4, pp. 231–242, Nov. 1996, doi: 10.1243/PIME_PROC_1996_210_462_02.

[3] X. Zhang, J. Li, and Y. B. Yin, 'Thermal Analysis and Simulation of Aircraft Hydraulic System', *Advanced Materials Research*, vol. 204, pp. 1984–1989, 2011, doi: https://doi.org/10.4028/www.scientific.net/AMR.204-210.1984.

[4] E. Busquets and M. Ivantysynova, 'Temperature Prediction of Displacement Controlled Multi-Actuator Machines', *International Journal of Fluid Power*, vol. 14, no. 1, pp. 25–36, Jan. 2013, doi: 10.1080/14399776.2013.10781066.

[5] L. Chenggong and J. Zongxia, 'Calculation Method for Thermal-Hydraulic System Simulation', *Journal of Heat Transfer*, vol. 130, no. 8, p. 084503, Aug. 2008, doi: 10.1115/1.2928006.

[6] K. Li, Z. Lv, K. Lu, and P. Yu, 'Thermal-hydraulic Modeling and Simulation of the Hydraulic System based on the Electro-hydrostatic Actuator', *Procedia Engineering*, vol. 80, pp. 272–281, 2014, doi: 10.1016/j.proeng.2014.09.086.

[7] S. Michel, 'Elektrisch-hydrostatische Kompaktantriebe mit Differentialzylinder für die industrielle Anwendung', PhD Thesis, 2021. [Online]. Available: https://doi.org/10.25368/2021.86.

[8] S. Ketelsen, S. Michel, T. O. Andersen, M. K. Ebbesen, J. Weber, and L. Schmidt, 'Thermo-Hydraulic Modelling and Experimental Validation of an Electro-Hydraulic Compact Drive', *Energies*, vol. 14, no. 9, p. 2375, Apr. 2021, doi: 10.3390/en14092375.

[9] H. Kwon, M. Sprengel, and M. Ivantysynova, 'Thermal modeling of a hydraulic hybrid vehicle transmission based on thermodynamic analysis', *Energy*, vol. 116, pp. 650–660, Dec. 2016, doi: 10.1016/j.energy.2016.10.001.

[10] Mohd. A. H. Siddiqui et al., 'Real-Time Comprehensive Energy Analysis of the LHD 811MK-V Machine with Mathematical Model Validation and Empirical Study of Overheating: An Experimental Approach', *Arab J Sci Eng*, vol. 47, no. 7, pp. 9043–9059, Jul. 2022, doi: 10.1007/s13369-021-06439-0.

[11] A. Al-Issa, T. Schulze, and J. Weber, 'An Improved Thermal Modelling Approach for Industrial Hydraulic System Applications, Prioritizing Computational Time Reduction and Thermal Condition Analysis', in *BATH/ASME 2024 Symposium on Fluid Power and Motion Control*, Bath, United Kingdom: American Society of Mechanical Engineers, Sep. 2024, p. V001T01A011. doi: 10.1115/FPMC2024-140068.

[12] Y. A. Çengel, *Heat Transfer: A Practical Approach*. McGraw-Hill, 2002.

[13] G. E. Totten and V. J. D. Negri, *Handbook of Hydraulic Fluid Technology*. CRC Press, 2011.

[14] W. Bock, 'Hydraulic Oils', in *Lubricants and Lubrication*, John Wiley & Sons, Ltd, 2017, pp. 345–420. doi: 10.1002/9783527645565.ch11.

[15] J. Zhang, N. Qi, and J. Jiang, 'Effect of Oil Viscosity on Hydraulic Cavitation Luminescence', *Fluid Dyn*, vol. 56, no. 3, pp. 371–382, May 2021, doi: 10.1134/S0015462821030125.

[16] P. Hodges, *Hydraulic Fluids*. Butterworth-Heinemann, 1996.

[17] S. Bair and P. Michael, 'Modelling the Pressure and Temperature Dependence of Viscosity and Volume for Hydraulic Fluids', *International Journal of Fluid Power*, vol. 11, no. 2, pp. 37–42, Jan. 2010, doi: 10.1080/14399776.2010.10781005.

[18] A. Al-Issa and J. Weber, 'Predicting Hydraulic Oil Thermophysical Properties Using Physics-Informed Neural Networks', *International Journal of Fluid Power*, pp. 59–88, Jul. 2024, doi: 10.13052/ijfp1439-9776.2513.

[19] W. Bock, 'Turbine Oils', in *Lubricants and Lubrication*, John Wiley & Sons, Ltd, 2017, pp. 453–490. doi: 10.1002/9783527645565.ch13.

[20] 'Axial Piston Variable Pump', Bosch Rexroth Hungary. Accessed: Oct. 04, 2024. [Online]. Available: https://www.boschrexroth.com/en/hu/media-details/861b3c0a-3169-49e2-9688-e71d02e2f4e5.

[21] F. Zhai, X. Wang, Z. He, Y. Chen, Z. Ye, and J. Yao, 'Analysis of Natural Heat Dissipation Capacity of Hydraulic Tank and Relevant Influencing Factors', *Machines*, vol. 10, no. 11, p. 991, Oct. 2022, doi: 10.3390/machines10110991.

[22] J. S. Cundiff, *Fluid Power Circuits and Controls: Fundamentals and Applications*, 0 ed. CRC Press, 2001. doi: 10.1201/9781420041330.

[23] M. Inc, 'Pilot Operated Servo Valves |D661 Series'. Accessed: Aug. 26, 2024. [Online]. Available: https://www.moog.com/products/servovalves-servo-proportional-valves/industrial/servo-and-proportional-valves-with-electronics/pilot-operated-servovalves-for-analog-signals-d661-series.html

[24] 'Emissivity - Metals |Fluke Process Instruments'. Accessed: Sep. 24, 2024. [Online]. Available: https://www.flukeprocessinstruments.com/en-us/service-and-support/knowledge-center/infrared-technology/emissivity-metals.

Biographies

Ahmad Al-Issa received the B.Sc. and M.Sc. degrees in mechanical engineering from AL-Mustansiriya University, Baghdad, Iraq in 2009 and 2012, respectively. This was followed by approximately 2 years as a university lecturer and then a 6-year industrial phase as a hydraulic engineer at General Company for Grain Processing, Ministry of Trade, Baghdad, Iraq. Currently, he is a research assistant and pursuing his PhD degree at Chair of Fluid-Mechatronic Systems, TU Dresden, Germany. His research focuses on thermal analysis and energy condition monitoring of complex industrial hydraulic systems. He is set to submit his PhD thesis on this topic later this year.

Tobias Schulze is working as a research associate and pursuing his Ph.D. at the Chair of Fluid-Mechatronic Systems (Fluidtronics) at TU Dresden, Germany. He serves as the team leader for the Fluid-Mechatronic Systems Group, with his research focusing on stationary hydraulic systems, specifically hydraulic deep drawing presses and electrohydraulic compact drives.

Jürgen Weber has been appointed in 1st March 2010 as a University Professor and the Chair of Fluid-Mechatronic Systems as well as the Director of the Institute of Fluid Power at TU Dresden, and took on the leadership of Institute of Mechatronic Engineering in 2018. He finished his doctorate in 1991 and was an active Senior Engineer at the former Chair of Hydraulics and Pneumatics until 1997. This was followed by a 13-year industrial phase. Besides his occupation as the Head of the Department Hydraulics and Design Manager for Mobile and Tracked Excavators, starting in 2002, he took on responsibility for the hydraulics in construction machinery at CNH Worldwide. From 2006 onwards, he was the Global Head of Architecture for hydraulic drive and control systems, system integration and advance development CNH construction machinery. Furthermore, Jürgen has been head of the Consulting Board for HYDAC, Sulzbach/Saar, for 10 years, still being a member, and was also appointed as a member of the Supervisory Board of Musashi Europe GmbH. He is a fellow and now chair of the Global Fluid Power Society. The membership of 5G Lab Germany at TU Dresden is a further indicator for more than 15 years of experience in management and coordination of research alliances as well as the activities as surveyor, PhD supervisor, over 300 publications, technical books and lecture notes.